NONLINEAR SEMBLANCE PROCESSING FOR THE EVALUATION OF AN ACOUSTIC ALTERED ZONE AROUND THE BOREHOLE

by

Kazuhiko Tezuka

Earth Resources Laboratory
Department of Earth, Atmospheric, and Planetary Sciences
Massachusetts Institute of Technology
Cambridge, MA 02139

and

JAPEX Research Center, Chiba 261, JAPAN

ABSTRACT

This paper describes a simple method to evaluate an acoustic altered zone around the borehole using an array of sonic waveforms. The method is based on a semblance velocity analysis and a nonlinear travel time window is introduced. On the assumption that a velocity gradient of the altered zone may be linear, the nonlinear travel time window is calculated as a function of averaged velocity and a normalized velocity gradient. The method is applied to the synthetic acoustic data calculated by finite difference modeling. Case studies with several altered formation models confirmed that this method is a good estimator of the velocity gradients around the borehole.

INTRODUCTION

Information about the acoustic velocity around the borehole is among the most important in exploration geophysics. In petroleum exploration this information is used to evaluate lithology, porosity, and the mechanical properties of the formation. Recent improvements in acoustic logging techniques enable us to get information not only for compressional velocity but also for shear and tubewave velocities. The multireceiver sonic tool estimates these velocities by using waveform arrays recorded at different source-receiver spacings. As those waveforms include elastic information along paths through which the waves have been propagated, there is a chance to investigate the velocity structure inside the formation.

Hornby(1992) detailed a method to reconstruct a two-dimensional slowness map of the formation using refracted borehole sonic data. Wu et al., (1993) calculated compressional and shear wave slowness using various combinations of subarrays and pointed out that acoustic alteration existed in the measured shear data, that is, the slowness from the receivers close-by is slower than that from the receivers far-off. From the com-

parison of VSP and sonic velocities, Tezuka and Takahashi (1993) reported that drilling induced alteration was one of the major causes for the negative drift (sonic velocity is slower than VSP velocity) in volcanic rocks. The elastic property of a formation near a borehole is altered by drilling, and drilling introduced stress relaxation. Microfractures around the borehole and borehole breakout are some of the phenomena caused by such alteration. For a further understanding of the elastic and stress conditions around the borehole it is important to know how deep and how severely the formation has been affected by drilling.

In this paper we describe a simple procedure to evaluate an acoustic altered zone. A modified semblance processing which has a non-linear scanning window is proposed and is applied to the synthetic acoustic logging data.

A LINEAR VELOCITY GRADIENT MODEL

We consider the two dimensional model of the formation (z, r) both radially away from the borehole and axially along the borehole (Figure 1). The acoustic altered zone between borehole and the fresh formation is assumed to have a linear gradient velocity structure. The velocity in the altered zone is

$$v(r) = v_0 + kr \tag{1}$$

where v_0 is the velocity at the borehole wall and k is a gradient of the velocity. Following the ray path theory an incident wave at point A is propagated along a bending ray path satisfying Snell's law

$$\frac{\sin\theta_0}{v_0} = \frac{\sin\theta}{v} \tag{2}$$

and

$$\frac{dz}{dr} = \tan\theta \tag{3}$$

where v is a velocity at the point (z, r) and θ_0 is an incident angle at the borehole wall. From equation (1) and (2) we get

$$dr = \frac{1}{k}\frac{v_0}{\sin\theta_0}\cos\theta d\theta. \tag{4}$$

Then the offset distance z is

$$\begin{aligned} z &= \int_0^z dz \\ &= \int_0^r \tan\theta dr \\ &= \int_{\theta_0}^{\theta} \frac{1}{k}\frac{v_0}{\sin\theta_0}\tan\theta d\theta \\ &= \frac{v_0}{\sin\theta_0}(\cos\theta_0 - \cos\theta) \end{aligned} \tag{5}$$

and the distance between A and D is

$$\begin{aligned} \overline{AD} &= \frac{2}{k}\frac{v_0}{\sin\theta_0}\int_{\theta_0}^{\frac{\pi}{2}}\sin\theta \\ &= \frac{v_0}{k}\cot\theta_0. \end{aligned} \tag{6}$$

By using the relation $v = ds/dt$ and equation (4), the short arc length ds is

$$\begin{aligned} ds &= \frac{dz}{\cos\theta} \\ &= \frac{v}{k}\frac{1}{\sin\theta}d\theta. \end{aligned} \tag{7}$$

Then the travel time from A to D is

$$\begin{aligned} t &= \int_0^t dt = \int_A^D \frac{1}{v}ds \\ &= 2\int_0^{z_m}\frac{1}{v\cos\theta}dz \\ &= \frac{2}{k}\int_{\theta_0}^{\frac{\pi}{2}}\frac{1}{\sin\theta}d\theta \\ &= \frac{2}{k}\sinh^{-1}(\cot\theta_0). \end{aligned} \tag{8}$$

Eliminating $\cot\theta_0$ from equation(8) with equation(6), we get the relation between t and z as follows

$$t = \frac{2}{k}\sinh^{-1}\left\{\frac{kz}{2v_0}\right\}. \tag{9}$$

Figure 2 (upper) shows the travel time against the offset distance with various velocity gradients. The parameters used in the calculation are: $v_0 = 3.0$km/s at $r = 0$ and a=0.0, 0.25, 0.5, 0.75 and 1.0. 'a' is a normalized velocity gradient

$$a = \frac{k}{v_0}.$$

The travel time curve becomes nonlinear as 'a' increases. The slope of the travel time curve at each offset represents the slowness at the deepest point in r by which the ray path can pass. Taking the derivative of t with respect to z, the slowness at the deepest point is

$$\frac{dt}{dz} = \frac{2}{\sqrt{k^2z^2 + 4v_0^2}}. \tag{10}$$

From equation(2) and (10), we get the penetration depth as follows

$$r_m = \sqrt{\left(\frac{z}{2}\right)^2 + \left(\frac{v_0}{k}\right)^2} - \frac{v_0}{k}. \tag{11}$$

Figure 2 (lower) shows the penetration depth at each offset distance. The same parameters are used for the calculation of travel times. The penetration depth depends on both the source-receiver offset and the velocity gradient. It deepens as both offset and gradient increase. However, it does not exceed half of the offset.

NON-LINEAR SEMBLANCE PROCESSING

The semblance processing is a powerful procedure to evaluate the velocity of each wave mode (compressional, shear, and Stoneley wave) from multireceiver sonic waveforms (Kimball and Marzetta, 1984). This method detects arrivals by computing the scalar semblance for a large number of possible arrival times and slownesses. The maxima of semblance are interpreted as arrivals and their associated slownesses. This method assumes that a formation is homogeneous over the span of the receiver array and uses a rectilinear window to compute the semblance (Figure 3). The detected slowness is considered to be the averaged slowness over the receiver array interval. For the linear gradient velocity model, the arrivals do not make a linear moveout, but an inverse hyperbolic moveout as shown in the equation (9). If the normalized gradient a is known, the maximum semblance value will be obtained with an appropriate window. Inversely, we can estimate a velocity gradient by trying to get the maximum semblance using a nonlinear window.

In conventional semblance processing, there are two scanning parameters of slowness and arrival time. In the nonlinear semblance method an additional unknown parameter of normalized velocity gradient a is required. As it is time consuming to calculate semblances over all the combinations of three scanning parameters, we reduce the number of parameters by adopting the results of conventional semblance processing. We assume that the averaged velocity, which is obtained by the conventional processing, represents the slope of the travel time curve at the mid point of the receiver array as follows

$$v_a = \frac{\sqrt{k^2 z_a^2 + 4v_0^2}}{2} \tag{12}$$

where v_a is an average velocity and z_a is a spacing between the source and the mid point of the receiver array. We fix the arrival time at z_a. In the actual configuration of sonic logging there is a delay on arrival time associated with the annulus of the fluid layer between the tool and the borehole wall. Strictly speaking, the delay time is different at each receiver. However, we neglect differences and assume the offset time to be constant. Then equation(9) should be modified as follows

$$t = \frac{2}{k} \sinh^{-1} \left\{ \frac{kz}{2v_0} \right\} + t_{ost}. \tag{13}$$

The fixed travel time at z_a can be written as

$$t_a = \frac{2}{k} \sinh^{-1} \left\{ \frac{kz_a}{2v_0} \right\} + t_{ost} \tag{14}$$

where t_{ost} is the constant offset time. Eliminating v_0 and t_{ost} from equations(12), (13), and (14), we get the travel time at each offset.

$$t(z) = \frac{\sqrt{a^2 z_a^2 + 4}}{a v_a} \left\{ \sinh^{-1} \left(\frac{az}{2} \right) - \sinh^{-1} \left(\frac{az_a}{2} \right) \right\} + t_a \tag{15}$$

This equation provides a nonlinear window for semblance processing. Figure 4 shows an example of non-linear moveout. The model used in this calculation is the one whose

averaged velocity is 4.88 km/s at the mid point of the receiver array. The spacing between the source and the mid point z_a is set to be 3.28m (10.75ft). The horizontal axis is a relative travel time, putting t_{ost} equal to zero. In nonlinear semblance processing, a number of semblances are calculated with various a, and the a that gives maximum semblance is interpreted as the normalized velocity gradient of the altered zone.

APPLICATION TO SYNTHETIC ACOUSTIC WAVEFORMS

To test the performance of nonlinear semblance processing, we applied this method to the synthetic acoustic waveforms. The synthetic waveforms are calculated by the finite difference modeling using a velocity - stress formulation on a staggered grid (Virieux, 1986; Kostek, 1990; Cheng, 1992). The models used in the test are 12.2-cm radius fluid-filled boreholes surrounded by elastic formations. The compressional velocity and density of the fluid are 1.61km/s and 1.30g/cm^3, respectively. The formation includes a linear velocity gradient acoustic altered zone between the borehole and the fresh formation. We used six models with different velocity gradients at the altered zone. The parameters and velocity structure of the models are shown in Table 1 and Figure 5, respectively. We put one point source and eight receivers at the center of the borehole and calculate eight waveforms. The shortest source-receiver spacing is 1.52m (5ft) and the longest is 4.72m (15.5ft). A 150*250 grid with $\Delta r = \Delta z = 3.048cm(0.1ft)$ is used. The time step is $\Delta t = 2\mu sec$. A Kelly source with a center frequency of 10kHz (Stephen et al., 1985) is applied as the source. A 50-grid point sponge layer is used as the absorbing boundary. Prior to the velocity analysis, we added to the waveforms some Gaussian noise whose variance is set to be -60dB of maximum waveform amplitude.

Figure 6 and 7 show the synthetic acoustic waveforms calculated for model-A and model-F. The synthetics of model-A, which has no altered zone, are showing typical acoustic logging waveforms with very small refracted P-wave arrival, relatively small S-wave arrival, and a significant amplitude of tube waves (Cheng and Toksöz, 1983). The straight moveouts of body waves and tubewaves are clearly observed. The synthetics of the most severely altered model (Figure 7) are rather complicated. The amplitude of the refracted P wave is bigger than that of model-A, because the contrast of acoustic impedance between fluid and borehole wall is smaller and much energy can be refracted at the boundary. With careful observation, a nonlinear moveout of the first arrival can be recognized. However, it is difficult to identify the refracted shear waves and tube waves from the following wavetrains. In this case the shear wave velocity at the borehole wall is lower than the fluid velocity and the shear velocity becomes rapidly higher than the fluid velocity in the vicinity of 23 cm from the interface. This condition causes an absence of refracted shear waves and makes the following wavetrains more complicated.

The complicated wavefield can be seen in a set of snapshots calculated with model-F (Figure 8). The snapshots show the vertical (z-axis) velocity field in a radius-depth space. The refracted P wave is clearly identified as the lowermost disturbance in the formation. Note the wavefront in the altered zone intersecting the borehole wall at approximately 45 to 60 degrees. From the intersecting point a compressional head wave is generated into the borehole.

The non-semblance processing is applied to these synthetic waveforms. First, we estimate averaged-velocity by using a linear semblance window. Then keeping v_a and t_a constant, sweeping a (normalized velocity gradient value) from 0 to 1.0, an appropriate value that would give the maximum semblance is looked for. The results for both the P- and S-wave are summarized in Table 2. The estimated normalized velocity gradients are plotted against the modeled value in Figure 8. We can see a good relationship between the modeled value and the estimated values. In the case of the P-wave, the relationship is almost linear. In the case of the S-wave, however, this method tends to estimate a lower value, especially in the higher range ($a > 0.5$). Because the S-wave velocities of a highly altered model are near to or lower than the fluid velocity, it becomes difficult to distinguish the refracted S-wave from the guided waves or the fluid wave. This contamination with another wave mode lowers the sensitivity when estimating the velocity gradient of an S-wave in high gradient cases.

Figure 10 shows the fit of the estimated velocity structures to those of the models. The dashed and dash-dot-dashed lines correspond to the P and S-wave velocity model. The filled circles and triangles correspond to the estimated P and S-wave structures. Three symbols on the lines represent the investigated depth and related velocity of the nearest, mid, and farthest receivers, respectively. Good agreement between estimated and modeled structures can be seen in most of the models not only for P-wave velocity structures but also for those of S-waves. Especially the averaged velocity, which is represented by symbols in the center, is plotted exactly on the modeled structure. This fact supports the correctness of the assumption that the averaged velocity represents the slope of the travel time curve at the mid point of the receiver array. The penetration depth depends not only on the source-receiver spacing, but also on the velocity structure. This is evident in Figure 9. We can get the velocity information inside the formation when the formation has a velocity gradient zone. It is concluded that this method can reconstruct the radial velocity structure for the case of simple altered zones, such as linear gradient velocity models.

CONCLUSION

This paper describes a simple method that can be used to evaluate an acoustic altered zone around the borehole. It is developed on the assumption that the altered zone has a linear velocity gradient. It evaluates a normalized velocity gradient by using modified semblance processing with nonlinear scanning time windows. Applying the method to several models confirms that this method is applicable to the evaluation of acoustic altered zones. For the case of simple altered zones, such as linear gradient velocity models, this method is regarded as a good estimator of both compressional and shear velocity in the structure around the borehole.

REFERENCES

Cheng, C.H., and M.N. Toksöz, 1981, Elastic wave propagation in a fluid-filled borehole and synthetic acoustic logs, *Geophysics, 46,* 1042–1053.

Cheng, N.Y., Zhu, C.H. Z., Cheng, and M.N. Toksöz, 1992, Experimental and finite difference modeling of borehole Mach waves, *M.I.T. Borehole Acoustics and Logging Consortium Annual Report.*

Hornby, B.E., 1992, Tomographic reconstruction of near borehole slowness using refracted borehole sonic arrivals, *62rd Ann. Int. Mtg., Soc. Expl. Geophys., Expanded Abstracts,* 70–74.

Kimball, C.V., and T.L. Marzetta, 1984, Semblance processing of borehole acoustic array data, *Geophysics, 49,* 274–281.

Kostek, S., 1990, *Modeling of elastic wave propagation in a fluid-filled borehole excited by a piezoelectric transducer,* M.S.Thesis, M.I.T., Cambridge, Mass.

Wu, P., D. Scheibner, and W. Rorland, 1993, A case of near-borehole shear velocity alternation, *Trans. Soc. Prof. Well Log Analysts 34th Ann. Logging Symp.,* paper R.

Tezuka, K., and A. Takahashi, 1993, Discrepancies between sonic log and VSP velocities in volcanic rocks, *63rd Ann. Int. Mtg., Soc. Expl. Geophys., Expanded Abstracts,* 715–718.

Virieux, J., 1986, P-SV wave propagation in heterogenous media: velocity-stress finite difference method, *Geophysics, 51,* 889–901.

Table 1. Model parameters

model ID	v_{0p} (km/s)	v_{0s} (km/sec)	ρ_0 (g/cm^3)	a_p	a_s
model-A	5.0	2.9	2.54	0.00	0.00
model-B	4.5	2.6	2.47	0.10	0.11
model-C	4.0	2.3	2.38	0.23	0.24
model-D	3.5	2.0	2.27	0.39	0.41
model-E	3.0	1.7	2.12	0.61	0.64
model-F	2.5	1.4	1.90	0.91	0.90

P wave velocity at borehole wall	v_{0p}: above
S wave velocity at borehole wall	v_{0s}: above
density at borehole wall	ρ_0: above
P wave velocity at fresh formation	v_{Cp}=5.0km/s
S wave velocity at fresh formation	v_{Cs}=2.9km/s
density of fresh formation	$\rho_C = 2.45$g/cm^3
fluid velocity	v_f=1.61km/s
fluid density	$\rho_f = 1.3$g/cm^3
borehole radius	r_b=0.12cm
outer altered zone radius	r_c=0.12cm

Table 2. Results of non-linear semblance processing

model ID	P-wave		S-wave	
	v_a (km/s)	a_p	v_a (km/s)	a_s
model-A	4.92	0.098	2.80	0.056
model-B	4.53	0.112	2.63	0.164
model-C	4.23	0.207	2.45	0.256
model-D	4.12	0.351	2.40	0.348
model-E	4.04	0.499	2.38	0.479
model-F	4.02	0.550	2.38	0.620

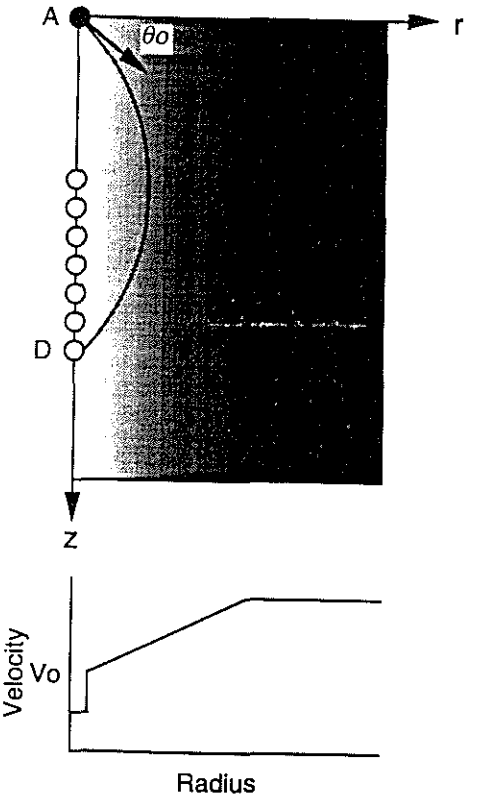

Figure 1: A two dimensional diagram showing acoustic logging in a formation that has a linear velocity gradient zone between the borehole and the fresh formation. This geometry is used for the finite difference simulation. A source is located at the origin (point A).

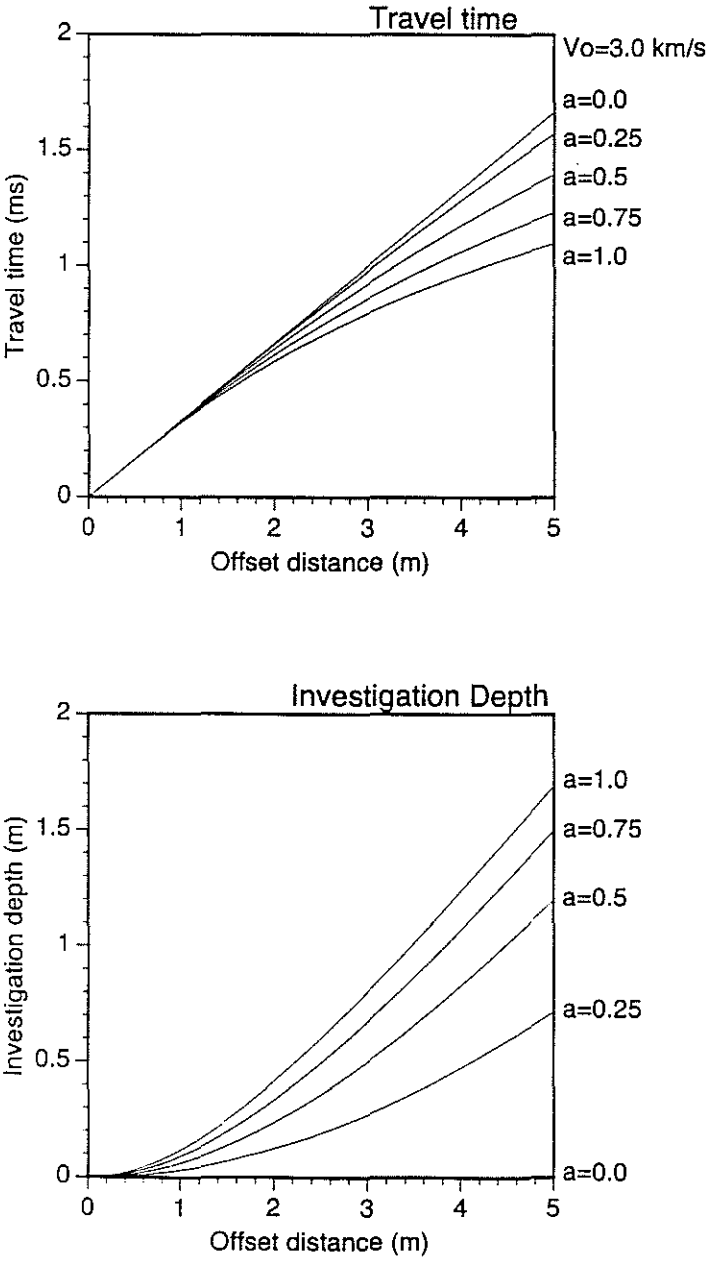

Figure 2: Travel time curves (upper) and penetration depth curves (lower) as a function of the source-receiver offset. Both curves are calculated for linear velocity gradient models. The normalized velocity gradients are 0.0, 0.25, 0.5, 0.75, and 1.0. Velocity at the borehole wall is v_0= 3.0 km/s.

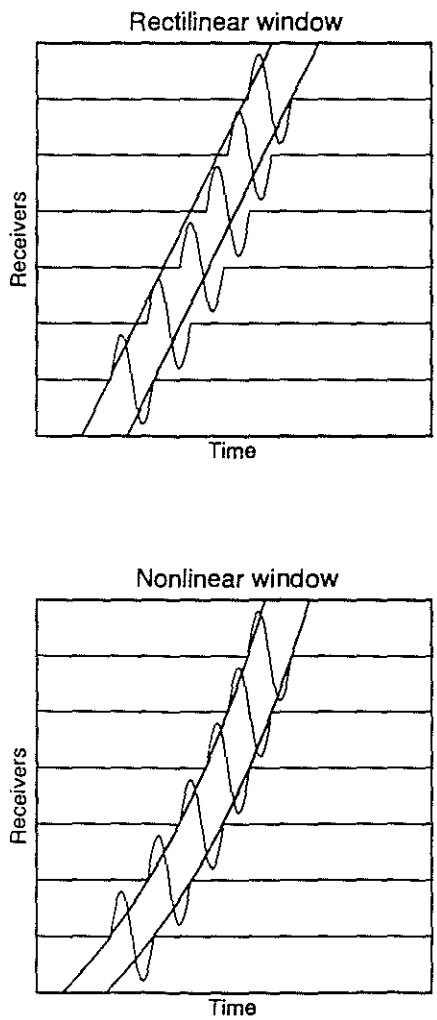

Figure 3: The rectilinear window for vonventional semblance processing (upper) and the nonlinear window used in the new method. Refracted wave arrivals which are propagated in the altered zone make a nonlinear moveout. The maximum value of semblance is obtained with an appropriate nonlinear window.

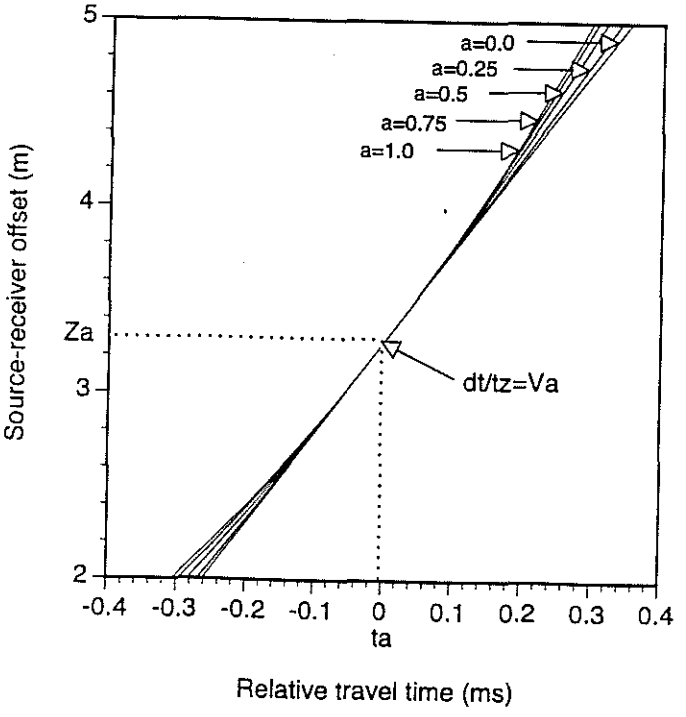

Figure 4: Moveout curves of the nonlinear windows whicha re used for nonlinear semblance processing. An averaged velocity at a mid-point of the receiver array (z_a = 3.28 m) is 4.88 km/s. Normalized velocity gradients are 0.0, 0.25, 0.5, 0.75, and 1.0.

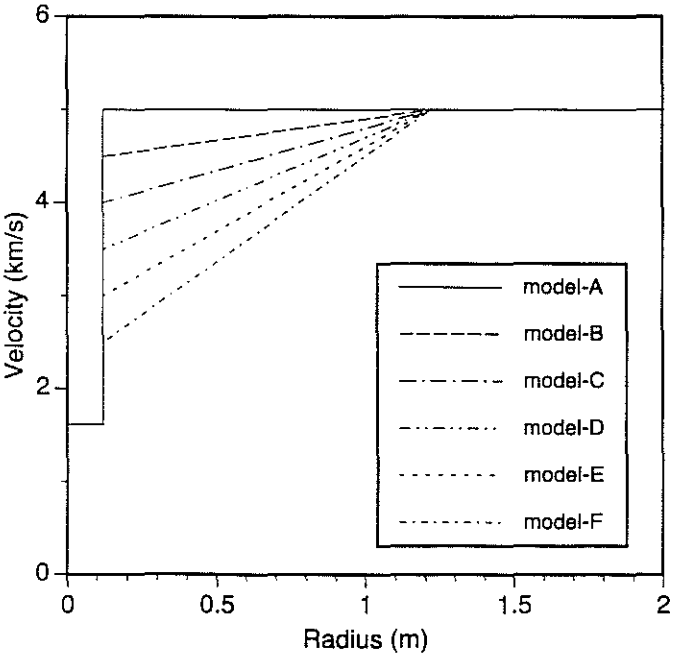

Figure 5: The P-wave velocity profile for linear velocity gradient models. These modles are representative of the acoustic altered formation. These parameters are also listed in Table 1.

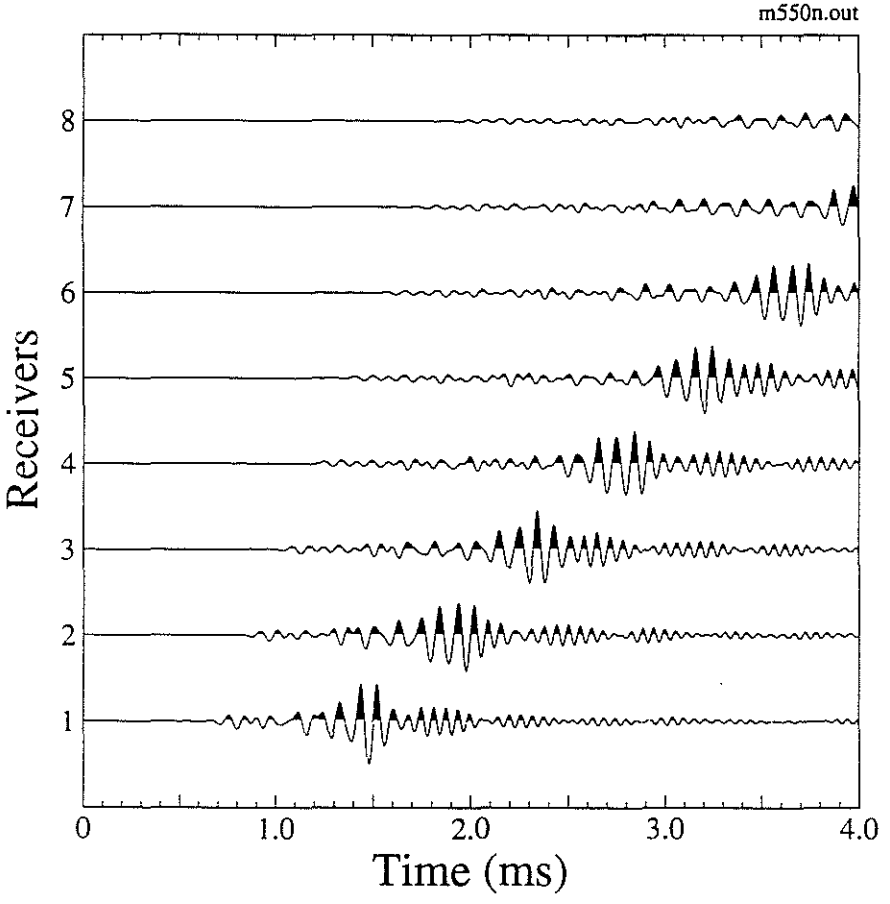

Figure 6: The synthetic waveforms calculated by the finite difference method for a non-altered zone model (model-A). Source-receiver offsets are from 1.52 m (5 ft) to 4.72 m (15.5 ft).

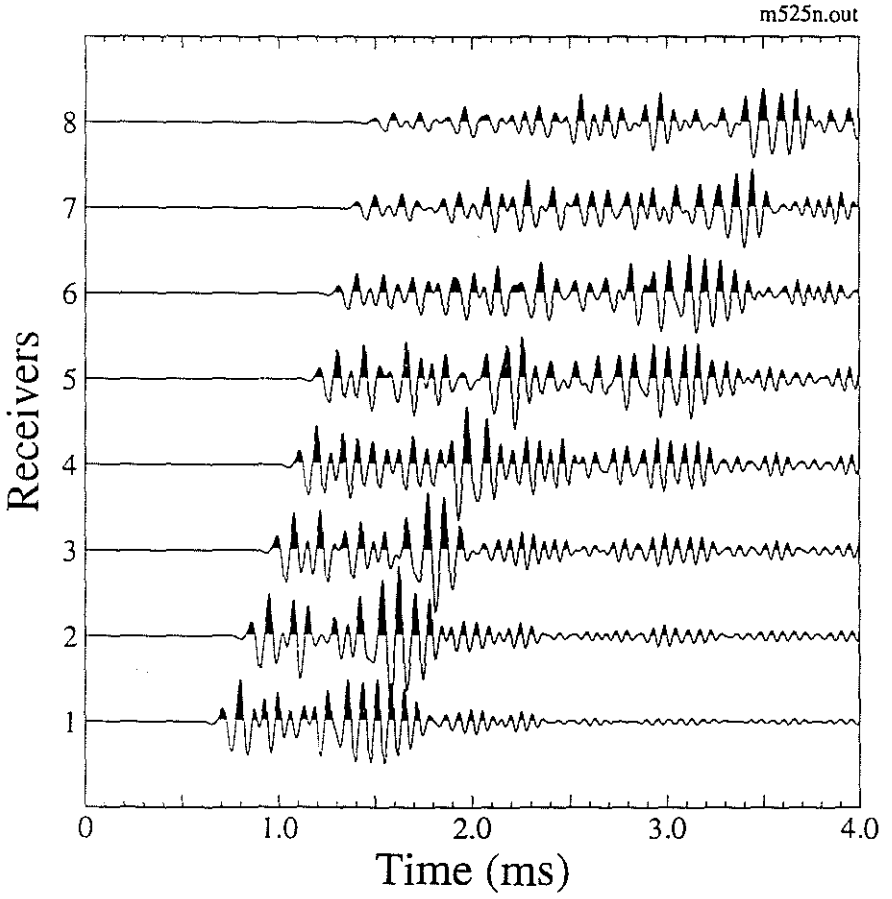

Figure 7: The synthetic waveforms calculated by the finite difference method for a severely altered zone model (model-F). Source-receiver offsets are from 1.52 m (5 ft) to 4.72 m (15.5 ft).

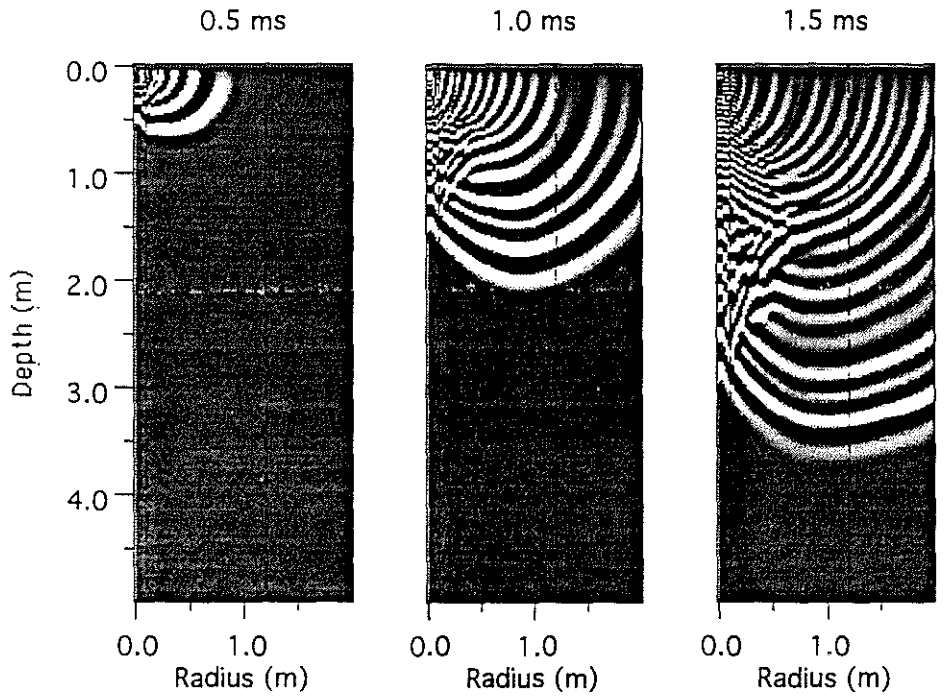

Figure 8: Snapshots of the wavefield calculated by the finite difference method for the most severely altered model (model-F). Each snapshot shows the amplitude distribution of the vertical velocity field in the radius-depth space. Time progresses from 0.5 ms to 1.5 ms.

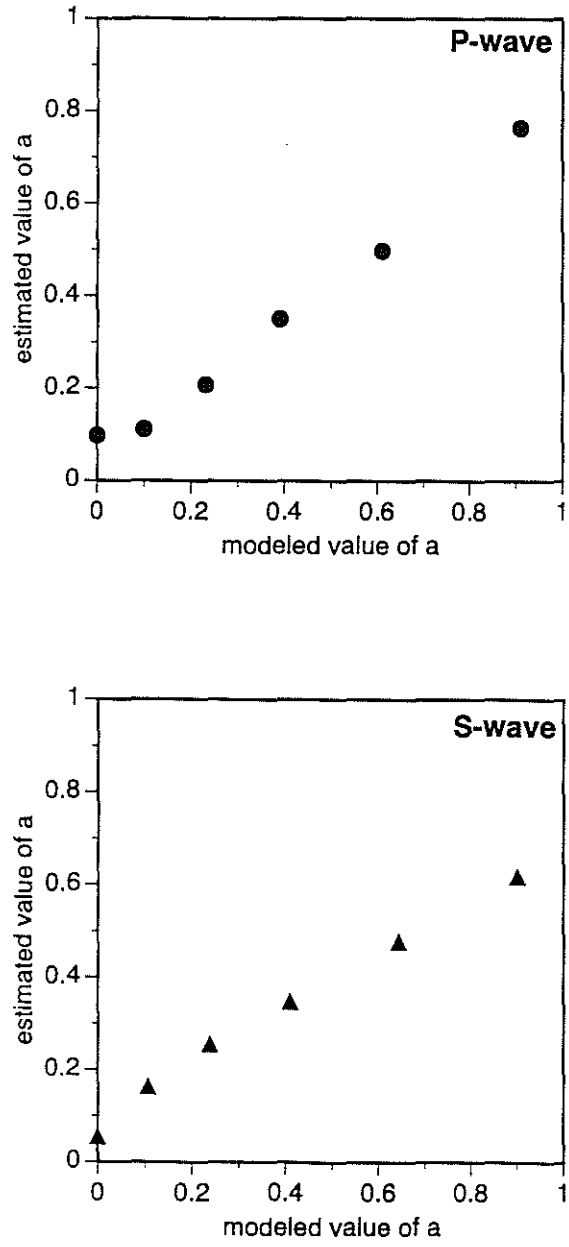

Figure 9: The plots of the estimated normalized velociti gradient against modeled values. There are good relationships between modeled and estimated values both in the P-wave (upper) and S-wave (lower) cases.

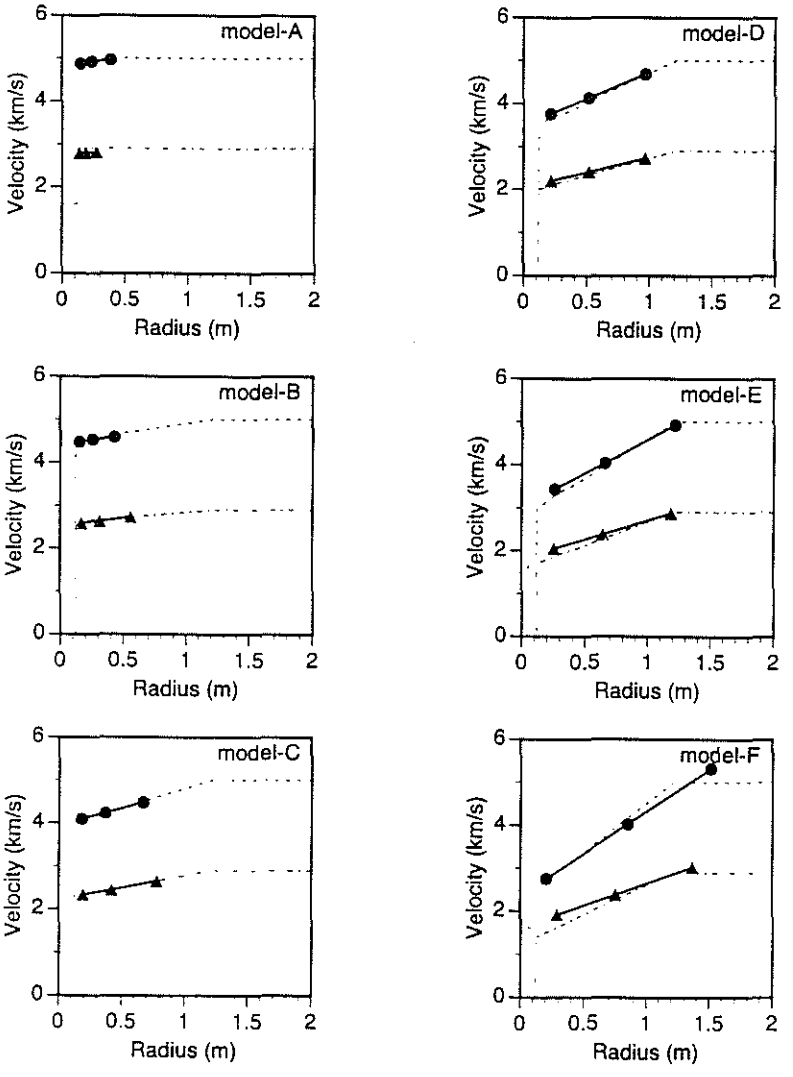

Figure 10: Fit of the estimated velocity structure to the model. The dashed and dash-dot-dash lines correspond to the P-wave and S-wave velocity model. The filled circle and filled triangle correspond to the estimated P- and S-wave velocity structure. Three symbols on the line represent the penetration depth and related velocity of the nearest, mid, and farthest receivers respectively.